Inducing periodicity and chaos by negative feedback

Elisabeth Pécou*, Bruno Cessac †‡§, Guillermo Espinoza¶

May 8, 2019

Abstract

Suppose that a parameter-dependent system has a stable equilibrium state for each parameter value in an interval and suppose that the equilibrium state has a first order dependence on the parameter. Basing ourselves on a mathematical result published earlier, we propose an algorithm to construct a negative feedback on the parameter which induces a Shilnikov or Lorenz type of chaos by building of homoclinic orbits. The algorithm is robust against variations of parameters and numerical uncertainty. One outcome is, for instance, in the Lorenz type of situation, trajectories visiting, in a chaotic order, neighborhoods of four given stable states of the initial system. We illustrate the results on the three-variables Goodwin model with negative regulation.

The second class of results presented here apply to a wider class of systems. Only supposing that a parameter-dependent system has stable states for two values of the parameter, we give a very simple feedback formula which allows us to obtain trajectories oscillating indefinitely between the stable states. The method is simulated on the three-variables Goodwin model with positive or negative regulation and low cooperativity index (< 8). The simulations show periodic orbits, which bifurcate by a cascade of period doubling when the distance between the stable states is varied, leading to chaos.

*Laboratoire J.-A. Dieudonné- UMR CNRS 6632 -Université de Nice Sophia Antipolis- Parc Valrose O6104 Nice cedex

†Team Odyssee, INRIA, 2004 Route des Lucioles, 06902 Sophia Antipolis, France

‡Université de Nice, Parc Valrose, 06000 Nice, France

§Institut Non Linéaire de Nice, UMR 6618 CNRS, 1361 route des Lucioles, 06560 Valbonne, France

¶Laboratoire J.-A. Dieudonné- UMR CNRS 6632 -Université de Nice Sophia Antipolis- Parc Valrose O6104 Nice cedex

In a previous paper it was showed how to induce self-disorganization inside a stable, parameter-dependent, system by adding a feedback on the parameter. Here we show that the method can be simulated in a numerical stable way. We apply with success the algorithm to the simplest differential equations model of a feedback loop regulatory structure, namely the Goodwin equations. Moreover we show theoretically how to induce periodic behaviour by adding a negative feedback, we propose a simulation algorithm and apply it to the Goodwin model with positive or negative regulation function.

1 Introduction and statement of results

In [1], it was proved that given a parametrized system of differential equations, that is a smooth family of smooth vector fields

$$\frac{dx}{dt} = F_\lambda(x) \quad x \in \mathbb{R}^n,\ \lambda \in]a,b[,$$

having a globally stable equilibrium state x^*_λ , it is possible to build a differential equation for the parameter such that the vector field $G = (g, F_\lambda)$ defined on $]a,b[\times\mathbb{R}^n$ by

$$\left\{ \begin{array}{l} \frac{d\lambda}{dt} = g(\lambda, x) \\ \frac{dx}{dt} = F_\lambda(x) \end{array} \right.$$

is chaotic. Moreover the proof gave a constructive method. See precise statement in Theorem 2.1.

The starting point of this paper is the motivation of applying this general method to large classes of systems, test the stability of the construction and observe the outcome. The first task has been to translate the method into a numerical algorithm (Section 3). We get, in a numerically stable way, the proved results in [1], that is Shilnikov type or Lorenz type of chaos depending whether the less contracting eigenvalue of linearized vector field at the stable point $x^*_{\lambda_0}$, $D_{x^*_{\lambda_0}} F_{\lambda_0}$, is real or complex. We have chosen to apply this algorithm to a classical model of stable system for genetic regulatory networks, namely the Goodwin model for negative regulation (Section 4). We have chosen as control parameters, first, the threshold value of the regulation fonction, and, second, the maximum reaction rate of the regulated component. In the Lorenz type of situation, a consequence of chaos is shown by trajectories which oscillate between four states in an unpredictable order, and moreover, this order is sensitive to initial conditions.

We prove, in Section 2, Theorem 2.2 which states that it is possible to proceed as follows. We choose two equilibrium states x^*_0 and x^*_1 with $r_0 = ||x_0|| < r_1 = ||x_1||$ corresponding to two different parameter values λ_0 and λ_1. We construct a feedback function g as a simple as a decreasing sigmoidal function of $r = ||x||$, which is positive close to r_0 and negative close to r_1. Then we obtain a system in which every orbit starting sufficiently close to x_0 (or x_1) oscillates indefinitly between x_0 and x_1.

For example, by adding this type of feedback to the parameter $V_{\max}$, the maximum reaction rate we create sustained oscillations with cooperativity index 4, see Fig. 8. This result is particularly interesting since it is known that the Goodwin model with negative regulation cannot exhibit oscillations when it applies to a three variable system with low "cooperativity index" (less than 8) (See [2] for instance for a detailed review on necessary conditions for oscillations in negative feedbacks).

Notice that this result applies to a wider class of systems than in Theorem 2.1. For instance, there might be bifurcation values in the interval $]\lambda_0, \lambda_1[$, like in bistable systems such as the Goodwin model with positive regulation.

Moreover, simulations show, in the case of the Goodwin model with positive or negative regulation a cascade of period doubling bifurcations, leading to chaos, obtained by varying the distance between the stable points.

2 Mathematical results

2.1 Chaos

For sake of completeness, we state here the theorem proved in [1].

Theorem 2.1 *Let $]a;b[\subset \mathbb{R}$ and $U \subset \mathbb{R}^n$ be open sets and let $\{ F_\lambda , \lambda \in]a;b[\}$ be a C^k-family of C^k-vector fields defined on U ($k \geq 1$, or $k = +\infty$). Assume that for each $\lambda \in I$, there exists $x^*_\lambda \in U$ which is a hyperbolic, globally attracting singularity for the differential equation:*

$$\frac{dx}{dt} = F_\lambda(x)$$

that is $F_\lambda(x^*_\lambda) = 0$, the Jacobian $J_\lambda = D_{x^*_\lambda} F_\lambda$ has all its eigenvalues with negative real parts, and the basin of x^*_λ contains U. Assume furthermore that

i) J_λ has only one real eigenvalue ρ with maximum negative real part or only one pair of complex conjugate eigenvalues $\rho \pm i\omega$ with maximum real part and

ii) there exists λ_0 such that

$$\partial_\lambda F_\lambda(x^*_\lambda)|_{\lambda=\lambda_0} \neq 0.$$

Then, there exists a C^∞-map $g : I \times U \to R$ such that the vector field $G(\lambda, x) = (g(\lambda, x), F_\lambda(x))$ is chaotic. More precisely, the flow of G has a homoclinic orbit and the first return map in a local section to the homocline has a countable set of horseshoes, and thus, a positive topological entropy.

Condition (i) is generic, and condition (ii) says that the vector field has an order 1 dependence on the parameter.

Sketch of the proof: The substance of the proof lies in the construction of a homoclinic orbit in the (λ, x)-phase space: we perturb the degenerated vector field $G_0 = (0, F_\lambda)$ so that a chosen stable singular point $M_0 = (\lambda_0, x^*_{\lambda_0})$ becomes a saddle singular point with a one-dimensional unstable manifold. Then, either one (or two) separatrix (separatrices) of M_0 are transformed into one or two homoclinic curve(s). Details can be found in [1], and the numerical building is explained in Section 3.

Once we have shown how to build a homoclinic orbit, the proof splits into two parts: (a) when the less contracting eigenvalue of the Jacobian J_{λ_0} is not real and has a complex conjugate eigenvalue (refered to as the "complex" case, or the Shilnikov-like situation); (b) when the less contracting eigenvalue of J_{λ_0} is real (this is the "real" case, or the Lorenz-like situation).

In the complex case, the existence of one homoclinic orbit directly implies the existence of chaos, like in the Shilnikov model of chaos (see [3],[4],[6]): the first return map to a cross section to the homoclinic orbit is shown to have an infinite number of horseshoes. In the real case, two homoclinic orbits are necessary, and after an arbitrary small perturbation, we get a Lorenz type of chaos with a strange attractor in the vicinity of the union of the homoclinic orbits. *QED*

Structural stability of the chaotic property The existence of a homoclinic orbit for a vector field is not structurally stable, but a small perturbation does not affect the chaotic behaviour as stated in the following proposition.

Proposition 2.1 *Given $\epsilon > 0$ small enough and given any C^k-map $g_\epsilon : I \times U \to R$, $\epsilon-$close to g, the flow of the vector field $G_\epsilon = (g_\epsilon, F_\lambda)$ admits a first return map to the local section Σ which has (at least) one horseshoe.*

Proof: In the real case, the construction is structurally stable, since it is obtained by an arbitrary perturbation of a non generic situation. It remains to treat the complex case. Consider a cross section Σ transverse to the homoclinic orbit and the first return map P_G to Σ of the flow of G. This map has a fixed point, which is the intersection of Σ with the homoclinic orbit. The general study of Shilnikov chaos (see for instance [6]) explains why the image of a rectangle R in Σ containing p in one of its edge spirals infinitely around p, creating infinitely many horseshoes. For a perturbation G_ϵ of G, the point p is not a fixed point anymore for the first return map P_{G_ϵ}, but its image $q = P_{G_\epsilon}(p)$ is close to p. With the same arguments as in the unperturbed situation, one can prove that the image of R spirals infinitely around q. As soon as q is sufficiently close to p, one can assert that the intersection of R with its image contains at least one horseshoe. See Fig 1.

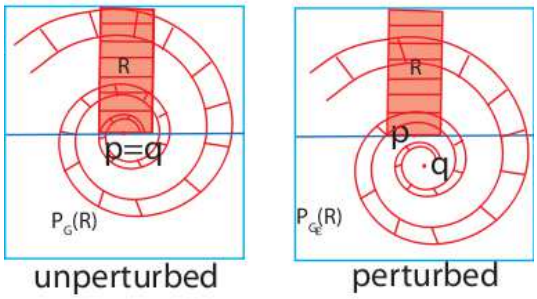

Figure 1: First return map of the unperturbed/perturbed Shilnikov type situation

QED

Chaotic oscillations The chaotic region is contained in a neighborhood of the homoclinic orbits, and this neighborhood might be small,

due to the specificities of the vector field F_λ. Then the chaotic behaviour might be diffficult to grasp simply by simulating trajectories. Nonetheless, a consequence of chaos at any scale can be attested when we are in a Lorenz-like situation. The following proposition recalls essential features of the chaotic vector field G built in this case. We keep the notations of Theorem 2.1.

Proposition 2.2 *Let λ_0 satisfy condition (ii) of Theorem 2.1 and suppose that the less contracting eigenvalue of the jacobian matrix J_λ is real for all $\lambda \in I$. Let λ_1, λ_2, λ_3 be in I and verify $\lambda_2 < \lambda_0 < \lambda_1 < \lambda_3$. Let $x_i^* = x_{\lambda_i}^*$ be the fixed point of F_{λ_i} and let $M_i = (\lambda_i, x_i^*)$ and V_i^ϵ an $\epsilon-$neighborhood of M_i in $\mathbb{R}^{n+1}$ for a given $\epsilon > 0$.*

Then, the chaotic vector field G has two homoclinic orbits H^+ and H^- such that H^+ intersects V_0^ϵ and V_1^ϵ and H^- intersects V_0^ϵ, V_2^ϵ and V_3^ϵ.

The proof of this proposition is contained in the proof of Theorem 2.1 in [1]. See Fig 2 that illustrates the construction of G.

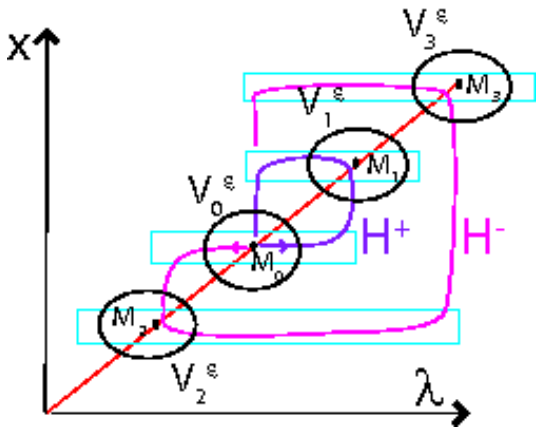

Figure 2: The vector field G in the real case

Proposition 2.3 *There exist tubular neighborhoods W^+ of H^+ and W^- of H^- such that $U_0 = W^+ \cap W^-$ is a neighborhood of M_0 and $W = W^+ \cup W^-$ is invariant by G: any orbit starting in W stays in W for all $t \in \mathbb{R}$.*

Notation: We denote by $B^k(x, r)$ the open ball with center x and radius r in $\mathbb{R}^k$ and $S^k(x, r)$ its bounding sphere.

Proof: (See Fig 3 and 4) Without loss of generality, we assume that $\lambda_0 = 0$ in $\mathbb{R}$ and $x_{\lambda_0}^* = 0$ in $\mathbb{R}^n$.

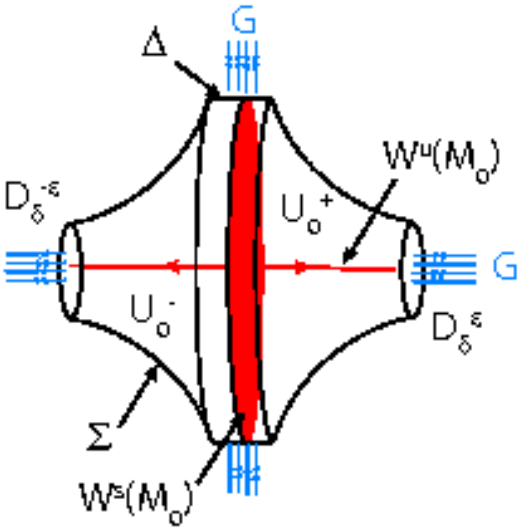

Figure 3: Invariant neighborhood U_0

We start by building an invariant neighborhood U_0 of the saddle M_0 (Fig 3). Let us consider ϵ_0 small enough so that G is topologically conjugated to its linear part inside the ball $B = B^{n+1}(M_0, \epsilon_0)$. We can then construct $U_0 \subset B$ assuming that G is linear. Consider two $n-$discs of diameter δ, $D_\delta^\epsilon = \{\epsilon\} \times B^n(0, \delta)$, and $D_\delta^{-\epsilon} = \{-\epsilon\} \times B^n(0, \delta)$ Let ψ_t be the flow of G, and consider the backward images of D_δ^ϵ in B: $U_0^+ = \bigcup_{t>0} \psi_{-t}(D_\delta^\epsilon) \cap B$ and of $D_\delta^{-\epsilon}$: $U_0^- = \bigcup_{t>0} \psi_{-t}(D_\delta^{-\epsilon}) \cap B$. Then, denoting by $W^s(M_0)$ the stable manifold of M_0,

$$U_0 = (U_0^+ \cup U_0^- \cup W^s(M_0)) \cap B$$

is a neighborhood of M_0 and its boundary is the union

$$\partial U_0 = \Pi \cup D \cup \Delta,$$

where Π is the boundary of $U_0^+ \cup U_0^-$, $D = D_\delta^\epsilon \cup D_\delta^{-\epsilon}$ and Δ is homeomorphic to a cylinder $]-\epsilon, \epsilon[\times S^n(0, \eta)$.

By construction, G is tangent to Π, transverse to D and outgoing, transverse to Δ and ingoing. Finally, any orbit crossing Δ and which is not contained is $W^s(M_0)$ crosses D in a future time. Notice that the previous construction is standard in topology.

Now, recall that $H^\pm$ denote the homoclinic orbits. We follow the $n-$discs $D_\delta^{\pm\epsilon}$ by the flow ψ_t of G for positive time $t > 0$. Since $H^\pm$ is a

hyperbolic orbit with a one dimensional unstable manifold, the union $T^{\pm} = \bigcup_{t>0} \psi_t(D_{\delta}^{\pm\epsilon})$ is a tubular neighborhood of $H^{\pm}$ in $(\mathbb{R}^{n+1} \setminus U_0)$, invariant by G (G is tangent to the boundary).

To conclude, we let $W^{\pm} = U_0 \cup T^{\pm}$. *QED*

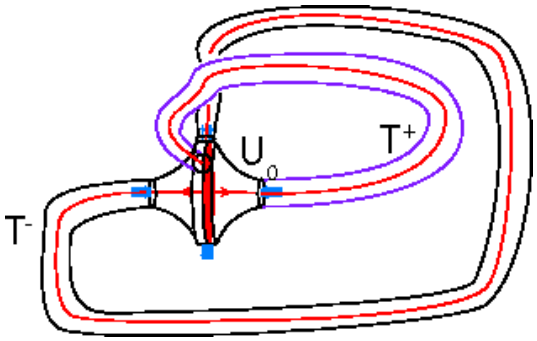

Figure 4: The neighborhoods $W^{\pm}$

A sequence of 0's and 1's can be associated to any orbit in W, which codes the order in which the orbit visits $T^{\pm}$ where, say, a 0 codes for the orbit visiting T^+ and a 1 codes for the orbit visiting T^-.

Proposition 2.4 *Any two distinct, arbitrarily close initial conditions have different codes.*

Proof: This is the expression of sensitivity to initial conditions, driven by the horseshoe(s). *QED*

As a conclusion one expects that the trajectory of the phase variable x, with an initial condition sufficiently close to x_0^* perpetually visits arbitrally small neighborhoods of the states x_0^*, x_1^*, x_2^*, x_3^* in an unpredictable order, and, moreover, this order is sensitive to initial conditions.

2.2 Periodic behaviour

Theorem 2.2 *Let $I \subset \mathbb{R}$ and let $\{F_\lambda, \lambda \in]a,b[\}$ be a C^k-family of C^k-vector fields defined on $\mathbb{R}^n$ ($n \geq 2$, $k \geq 1$, or $k = +\infty$). Assume that there exist λ_0 and λ_1 in $]a,b[$ such that F_{λ_i} has a hyperbolic globally attracting singularity $x_i^* \in \mathbb{R}^n$ ($i = 0, 1$). Let $M_0 = (\lambda_0, x_0^*)$ and $M_1 = (\lambda_1, x_1^*)$.*

Then, there exist a C^∞-map $g : I \times \mathbb{R}^n \to R$, such that M_0 and M_1 are hyperbolic saddle fixed points for the vector field $G(\lambda, x) = (g(\lambda, x), F_\lambda(x))$ and for arbitrarilly small invariant neighborhoods U_0 and U_1 of M_0 and M_1 respectivelly such that all orbits of G crossing $U_0^+ = U_0 \cap]\lambda_0, \lambda_1[\times \mathbb{R}^n$ or $U_1^- = U_1 \cap]\lambda_0, \lambda_1[\times \mathbb{R}^n$ visits alternatively U_0^+ and U_1^- for all time.

Proof: To simplify the notations, let $(\lambda_0, x_0^*) = (0,0)$. Choose $\delta > 0$ such that both cylinders $C_0 = [0, \lambda_1] \times B^n(0, \delta)$ and $C_1 = [0, \lambda_1] \times B^n(x_{\lambda_1}^*, \delta)$ do not intersect.

Since the property of having a hyperbolic globally attracting singularity is structurally stable, there exists $\epsilon > 0$ so that for each $\lambda \in]-\epsilon, \epsilon[$ or $\lambda \in]\lambda_1 - \epsilon, \lambda_1 + \epsilon[$, F_λ keeps this property.

First step. Suppose that there exists a map g defined for $(\lambda, x) \in [0, \lambda_1] \times \mathbb{R}^n$ such that:

(H1) M_0 and M_1 are saddle hyperbolic fixed points for $G = (g, F_\lambda)$ and $W^s(M_i) = \{\lambda_i\} \times \mathbb{R}^n$.

Let ψ_t be the flow of G.

Like in the previous section (proof of Proposition 2.3), we construct "half-neighborhoods" U_0^+ and U_1^- of the saddle points M_0 and M_1.

Consider, for $\epsilon_0 \leq \epsilon$ small enough and $\eta_0 < \delta$, the $n-$disc $D^+ = \{\epsilon_0\} \times B^n(0, \eta_0)$. Let

$$V_0^+ = \bigcup_{t>0} \psi_{-t}(D^+),$$

$U_0^+ = V_0^+ \cap C_0$ and $\Pi^+ = V_0^+ \cap \partial C_0$.

In a similar way, we define, for $\epsilon_1 \leq \epsilon$ small enough and $\eta_1 < \delta$, $D^- = \{\lambda_1 - \epsilon_1\} \times B^n(x_1^*, \eta_1)$. Let $V_1^- = \bigcup_{t>0} \psi_{-t}(D^-)$, $U_1^- = V_1^- \cap C_1$ and $\Pi^- = V_1^- \cap \partial C_1$.

The following lemma holds readily.

Lemma 2.1 *The vector field G is tangent to the boundary of U_0^+ and U_1^-. G is transverse to $\Pi^+ \cup D^+$ and to $\Pi^- \cup D^-$ and the flow ψ_t enters U_0^+ (resp. U_1^-) through Π^+ (resp Π^-) and leaves U_0^+ (resp. U_1^-) through D^+ (resp D^-). Finally, each orbit crossing Π^+ (resp Π^-) has to cross next D^+ (resp D^-).*

For $\zeta_1 > 0$ small enough, $V_1^- \cap C_0$ contains a cylinder $]\lambda_1 - \zeta_1, \lambda_1[\times B^n(0, \delta)$. Consider a conic hypersurface K_0 with axis $\{x = 0, \lambda \in [\epsilon_0, \lambda_1 - \zeta_1]\}$, and bounded by the $n-$discs D^+ and $\{\lambda_1 - \zeta_1\} \times B^n(0, \delta)$.

Similarly, there exists $\zeta_0 > 0$ small enough such that $V_0^+ \cap C_1$ contains $]0, \zeta_0[\times B^n(x_1^*, \delta)$. We let K_1 be a conic hypersurface with axis $\{x = x_1^*, \lambda \in [\zeta_0, \lambda_1 - \epsilon_1]\}$, and bounded by the $n-$discs D^- and $\{\zeta_0\} \times B^n(x_1^*, \delta)$.

We define $\mathbf{K}_i$ the volume bounded by K_i, $i = 0, 1$.

Suppose that g satisfies moreover that

(H2) G is transverse and ingoing to K_0 and K_1.

Consider a point of D^+. Its future orbit by ψ_t stays in $\mathbf{K_0}$, then crosses $\{\lambda_1 - \zeta_1\} \times B^n(0, \delta)$, enters V_1^-, crosses Π^- and finally intersects D^-. Since the previous construction is symetric, it is clear that the flow ψ_t induces a map from D^- to D^+. By composing both maps we get a well defined first return map on D^+. Moreover, the orbit of a point in U_0^+ crosses alternatively D^+ and D^- for all future time.

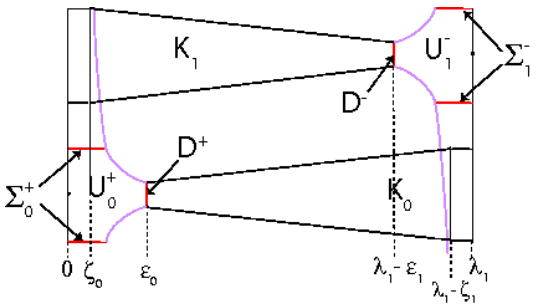

Figure 5: Trapping region

Second step Let us construct a map g that satisfies hypothese (H1) and (H2).

Let us define the family of step functions:

$$\sigma_{a,k}(r) = \frac{a^k - r^k}{a^k + r^k}, \quad a > 0,\ k \in \mathbb{N},\ r > 0$$

Those functions decrease from 1 to -1 and vanish at $r = a$. The derivative is 0 at $r = 0$ and tend to 0 when $r \to +\infty$. The steepness of the curve at $r = a$ increases with k.

Lemma 2.2 *There exist k and μ such that one can choose $a = ||x_1^*||/2$ and*

$$g(\lambda, x) = \begin{cases} \mu\lambda(\lambda_1 - \lambda)\sigma_{a,k}(||x||) & \text{if} \quad \lambda \in [0, \lambda_1] \\ 0 & \text{if} \quad \lambda \,\text{else} \end{cases}$$

g satisfies (H1): Notice that $g(0,0) = g(\lambda_1, x_1^*) = 0$, and thus M_0 and M_1 are equilibrium points of the vector field G. A straightforward computation gives:

$$\frac{\partial g}{\partial \lambda}(0,0) = \mu\lambda_1 \quad \frac{\partial g}{\partial \lambda}(\lambda_1, x_1^*) = \mu\lambda_1 \frac{2^k - 1}{2^k + 1}$$

and

$$D_x g(0,0) = 0 \quad D_x g(\lambda_1, x_1) = 0$$

As a consequence, the eigenvalues of $D_{(\lambda,x)}G(M_0)$ are those of $D_x F_0(0)$ and $\mu\lambda_1$. Similarly, the eigenvalues of $D_{(\lambda,x)}G(M_1)$ are those of $D_x F_{\lambda_1}(x_1^*)$ and $\mu\lambda_1 \frac{2^k-1}{2^k+1}$. Thus M_0 and M_1 are hyperbolic points with a one dimensional unstable manifold. Moreover, since $g = 0$ on $\{0\} \times \mathbb{R}^n$, the stable manifold of M_0 is $W_s(M_0) = \{0\} \times \mathbb{R}^n$. For the analogous reason, $W_s(M_1) = \{\lambda_1\} \times \mathbb{R}^n$.
For μ large enough, g satisfies (H2): We show that there exists $\mu > 0$ large enough so that G is transverse to the boundary of the cone K_0 and directed inside the cone. Denoting α the slope of K_0, this condition is satisfied as soon as for any $(\lambda, x) \in K_0$,

$$\alpha g(\lambda, x) > ||F_\lambda(x)||$$

Let $\bar{\lambda} = \min(\epsilon_0, \zeta_1)$; then for $\lambda \in [\epsilon_0, \lambda_1 - \zeta_1]$ we have $\lambda(\lambda_1 - \lambda) \geq \bar{\lambda}(\lambda_1 - \bar{\lambda})$. On the other hand, for $x \in B^n(0, \delta)$,

$$\sigma_{||x_1^*||/2,k}(||x||) \geq \sigma_{||x_1^*||/2,k}(||\delta||)$$

. Thus g is minored on K_0 by:

$$g(\lambda, x) \geq C\mu$$

where

$$C = \bar{\lambda}(\lambda_1 - \bar{\lambda})\sigma_{||x_1^*||/2,k}(||\delta||)$$

By letting

$$\mu \geq \frac{1}{\alpha C} \sup\{||F_\lambda(x)||\,,\ (\lambda, x) \in K_0\}$$

the corresponding vector field G points inward the cone K_0.

In the same way, there exist μ such that G points inward the cone K_1 and hypothesis (H2) is satisfied. *QED*

3 Numerical realization

3.1 Algorithm (I): inducing chaos by homoclinic orbits

3.1.1 Algorithm.

The constructive proof of Theorem 2.1 provides a straightforward algorithm allowing the desynchronization of a large class of dynamical systems. The implementation of this algorithm does not require a detailed knowledge of the dynamics, and the modified vector field is constructed step by step, by following a given trajectory.

We are attempting to construct a function $g(\lambda, x)$, where x is a point in the phase space and λ a control parameter, such that the extended dynamical system:

$$\left\{ \begin{array}{rcl} \frac{d\lambda}{dt} & = & g(\lambda, x) \\ \frac{d\mathbf{x}}{dt} & = & \mathbf{F}(\lambda, \mathbf{x}) \end{array} \right. \quad (3.1)$$

has a homoclinic orbit.

In [1] it is shown that this can be obtained by constructing g as a juxtaposition of elementary functions, called "dynamical blocks", which have the form:

$$B_{M,a,b,\mu,\delta}(R) = \frac{(\lambda - \lambda_M)(b-\lambda)^2(a-\lambda)^2}{(b-\lambda_M)^2(a-\lambda_M)^2} h_{\mu,\delta}(R) \quad (3.2)$$

where $M = (\lambda_M, x_M)$ is a stable fixed point, and a, b two real parameters called the left and right "horizontal size" of the block. The function $h_{\mu,\delta}$ is given by:

$$h_{\mu,\delta}(R) = \left\{ \begin{array}{cc} \frac{\mu}{2}\left[1 + \cos\left(\frac{\pi R^2}{\delta^2}\right)\right] & \text{if} \quad R \leq \delta \\ 0 & \text{if} \quad R > \delta \end{array} \right. \quad (3.3)$$

where $R = \|x - x_M\|$ and where μ, δ are 2 positive real numbers respectively called the radius of the block, and the injection speed. Thus, a block is a cylinder, and $B_{M,a,b,\mu,\delta}$ is zero outside the block.

Now, for a suitable choice of parameters a,b,δ and μ, one can render the singular point M unstable, with an unstable manifold almost parallel to the direction λ in the neighborhood of M, and the vector field projection on this direction is quite larger than the projection on the other directions. Therefore, a small perturbation about M is driven by the flow away from M with a speed almost parrallel to the λ axis. By construction the amplitude of this speed decreases when moving away from M, and it vanishes at the boundaries of the cylinder, where the flow is orthogonal to the direction (O, λ). Constructing g as an assembly of suitable blocks one can manage that M is a homoclinic point for the modified vector field.
In the following, we construct the perturbed vector field in a simple example.

3.1.2 Constructing the blocs. An example.

Consider the dynamical system:

$$\left\{ \begin{array}{rcl} \frac{dY}{dt} & = & (-1+\lambda)\left(\alpha(Y-\lambda) + \beta Z\right) \\ \frac{dZ}{dt} & = & (-1+\lambda)\left(-\beta(Y-\lambda) + \alpha Z\right) \end{array} \right. \quad (3.4)$$

It is linear, with a fixed point $X^* = (Y = \lambda, Z = 0)$. It is stable if $\lambda < 1, \alpha > 0$, and this is a focus if $\beta < 0$.

We would like to desynchronize this system, with the block construction discussed above. We thus consider the modified vector field:

$$\left\{ \begin{array}{rcl} \frac{d\lambda}{dt} & = & g(\lambda, Y, Z) \\ \frac{dY}{dt} & = & (-1+\lambda)\left(\alpha(Y-\lambda) + \beta Z\right) \\ \frac{dZ}{dt} & = & (-1+\lambda)\left(-\beta(Y-\lambda) + \alpha Z\right) \end{array} \right. \quad (3.5)$$

In the sequel we fix $\alpha = 1, \beta = -4$. Call $\Gamma = \{\lambda, \lambda, 0\}$. This is the set of fixed points for (3.4) when λ varies.

We add a first bloc $B_{M,a,b,\mu,\delta}(R)$ located at $M = O_1 = (\lambda = 0, X = 0, Y = 0)$ and symetric with respect to this point (Fig. 6). We fix $\delta = 0.05, \mu = 100$. We slightly perturb M. This point is now unstable. Its trajectory moves away from M and is roughly parrallel to the λ axis until the trajectory reaches the boundary of the bloc. Then it moves verticaly and eventually reaches the line of fixed points Γ. Then it converges to a new fixed point O_2.

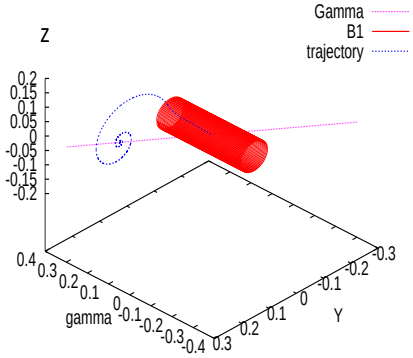

Figure 6: Effect of the first bloc on a trajectory of (3.5) starting in a neighbourhood of M

We now choose this fixed point as the center of a second bloc and the left horizontal size is such that the left border of the bloc is just above O_1, -$a_2 = 0$).

Thus 0_2 becomes unstable and a suitable choice of a_2 allows the trajectory of a small perturbation of O_2 (its unstable manifold) to come arbitrary close from 0_1. But then the trajectory

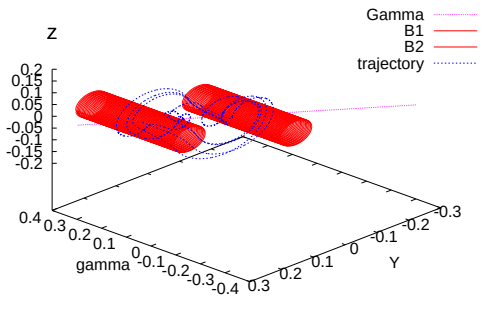

Figure 7: Effect of the first bloc on a trajectory of (3.5) starting in a neighbourhood of O_1

feels the first bloc, and moves away from 0_1. It eventually enters in the second block, etc..

3.2 Algorithm (II): inducing periodicity

This case corresponds to Theorem2.2. We simulate the system using the analytical expression of the feedback function g given in Lemma 2.2, which only depends on the initially chosen fixed points M_0 and M_1, and on a parameter μ which is adjusted by numerical experiments.

4 Chaotization of the Goodwin model

The Goodwin equations (see [5]) model a feedback circuit (positive or negative):

$$\begin{aligned} \frac{dx_1}{dt} &= K_1 C R^{\pm}_{\theta,m}(x_n) - \gamma_1 x_1 \\ \frac{dx_2}{dt} &= K_2 x_1 - \gamma_2 x_2 \\ &\dots \\ \frac{dx_n}{dt} &= K_n x_{n-1} - \gamma_n x_n \end{aligned}$$

They are the simplest equations in the sense that the unique nonlinear term is the regulation function which is sigmoidal, increasing or decreasing, with a threshold θ and cooperativity index m:

$$R^{+}_{\theta,m}(z) = \frac{1+z^m}{z^m+\theta^m} \quad R^{-}_{\theta,m}(z) = \frac{\theta^m}{z^m+\theta^m}$$

We let $V_{\max} = K_1 C$ be the maximum reaction rate giving x_1.

4.1 Goodwin equations with negative feedback

4.1.1 Oscillations

Fig. 8 illustrates the use of Algorithm (II) on the negative Goodwin model when the feedback is made on the threshold θ. In Fig. 9 , the feedback is made on the maximum reaction rate $V_{\max} = K_1 C$.

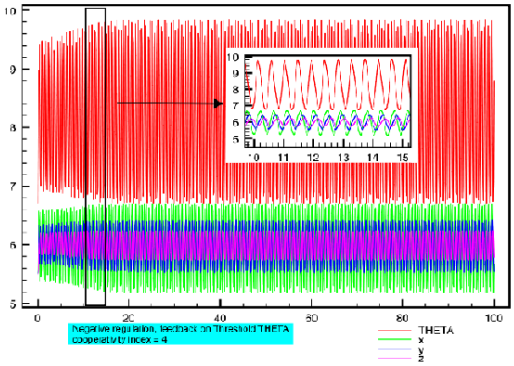

Figure 8: Oscillations in the negative Goodwin model with $n = 3$ variables and cooperativity index $m = 4$. The feedback is made on θ. Other parameters are: $V_{\max} = K_1 C = 80\,\mathrm{Mol}.l^{-1}t^{-1}$, $K_2 = K_3 = \gamma_1 = \gamma_2 = \gamma_3 = 10\,t^{-1}$. The algorithm runs with μ between 29 (picture) and 35 (see section 3).

4.1.2 Chaos

We use Algorithm (II). By varying the distance between the initially chosen stable states, we observe a cascade of period doubling bifurcation of periodic orbits, like in Fig. 10.
We use Algorithm (I). We obtain a Lorenz type of chaos by constructing two homoclinic orbits. Parameters of the Goodwin model are chosen in order to have only real negative eigenvalues at the chosen initial state.

It is important to emphasize that obtaining chaos depends on the fine tuning of a certain parameter to be the closest possible to the homoclinic situation. This fine tuning can be difficult to do numerically, and it is reasonnable, in practical, to ask for a transient chaotic behaviour over a sufficiently large period, instead of permanent chaos.

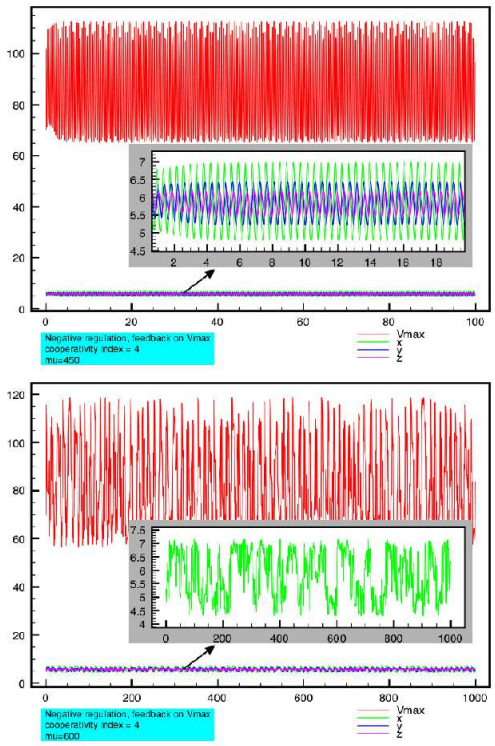

Figure 9: Oscillations in the negative Goodwin model with $n = 3$ variables and cooperativity index $m = 4$. The feedback is made on $V_{\max}$. Other parameters are:$\theta = 7\,\text{Mol}.l^{-1}$, $K_2 = K_3 = \gamma_1 = \gamma_2 = \gamma_3 = 10\,t^{-1}$. The algorithm runs with μ between 409 and 608. The simulations shown are for $\mu = 450$ (up), and $\mu = 600$ (down) (see section 3).

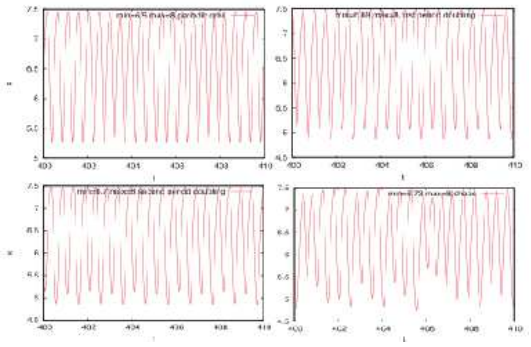

Figure 10: Cascade of period doubling bifurcation of periodic orbits in the negative Goodwin model with $n = 3$ variables and cooperativity index $m = 4$. Other parameters are: $V_{\max} = K_1 C = 80\,\text{Mol}.l^{-1}t^{-1}$, $K_2 = K_3 = \gamma_1 = \gamma_2 = \gamma_3 = 10\,t^{-1}$, $\mu = 29$.

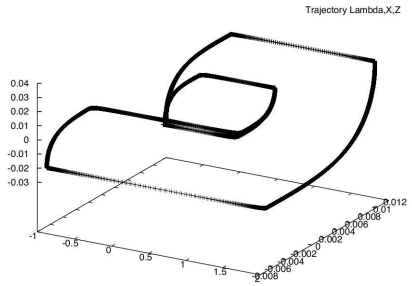

Figure 11: Chaotic behaviour in the negative Goodwin model with $n = 4$ variables and cooperativity index $m = 4$. Other parameters are: $V_{\max} = K_1 C = 0.32\,\text{Mol}.l^{-1}t^{-1}$, $\theta = 20\,\text{Mol}.l^{-1}$, $K_2 = K_3 = 0.32\,t^{-1}$, $\gamma_1 = 0.17\,t^{-1}$, $\gamma_2 = 0.18\,t^{-1}$, $\gamma_3 = 0.19\,t^{-1}$. The chosen fixed points are those corresponding to $\theta = 19, 20, 21, 22\,\text{Mol}.l^{-1}$. Other parameters are (see Section 3) $\mu = 0.002$, $\epsilon = 0.03$, $la = 0.02$

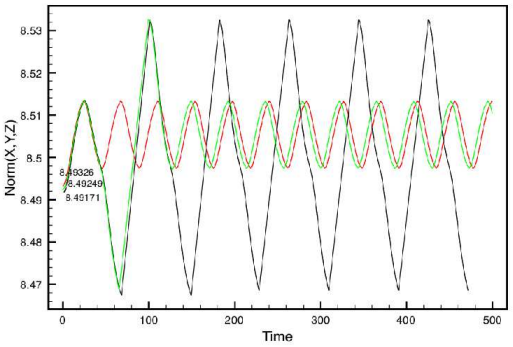

Figure 12: Chaotic behaviour in the negative Goodwin model: sensitivity is illustrated on three close initial conditions. Parameters are the same as in Fig 11.

4.2 Goodwin equations with positive feedback

4.2.1 Oscillations

Fig. 13 illustrates the use of Algorithm (II) on the positive Goodwin model.

4.2.2 Chaos

We use Algorithm (II). By varying the distance between the initially chosen stable states, we ob-

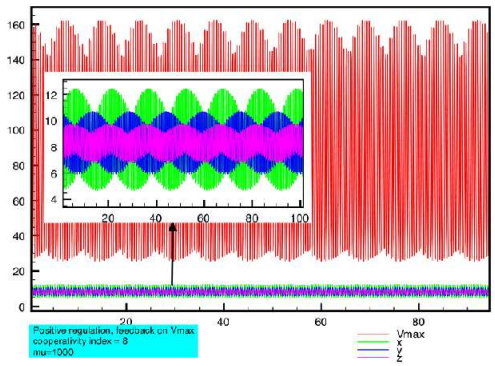

Figure 13: Oscillations in the positive Goodwin model with $n = 3$ variables and cooperativity index $m = 8$. The feedback is made on $V_{\max}$. Other parameters are: $\theta = 10\,\mathrm{Mol}.l^{-1}$, $K_2 = K_3 = \gamma_1 = \gamma_2 = \gamma_3 = 10\,t^{-1}$. The algorithm runs withμ between 694 and 1087 ($\mu = 1000$ in the simulation shown).

serve a cascade of period doubling bifurcation of periodic orbits, like in Fig. 14.

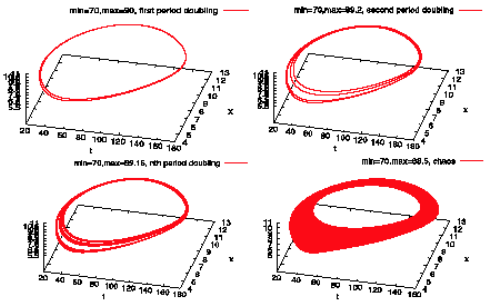

Figure 14: Cascade of period doubling bifurcation of periodic orbits in the positive Goodwin model with $n = 3$ variables and cooperativity index $m = 8$. The feedback is on $V_{\max}$. Other parameters are: $\theta = 10\,\mathrm{Mol}.l^{-1}$, $K_2 = K_3 = \gamma_1 = \gamma_2 = \gamma_3 = 10\,t^{-1}$ and $\mu = 1000$.

5 Conclusions and perspectives

We have constructed negative feedbacks on the Goodwin model equations in four cases:

1. Negative regulation system and the feedback is made on the parameter a) the threshold θ; b) the maximum reaction rate $V_{\max}$,
2. Positive regulation system and the feedback is made on the parameter a) the threshold θ (not shown); b) the maximum reaction rate $V_{\max}$.

A first class of results was obtained by using very simple forms of feedback functions: alternatively positive and negative step-like functions. In each case, we obtained oscillations between two arbitrary, globally stable, states of the initial parametrized system (the reference states). The explanation is that there exists a trapping tubular region for the extended vector field containing both reference states in the enlarged phase space, and orbits in this torus are forced to go the way around for ever. Naturally, it is well known that negative feedbacks are necessary conditions for oscillations: in our paper we give a way to construct the negative feedback to effectively get oscillations in a parametric family of stable systems. Moreover, oscillations are built between two chosen (initially stable) states and might be larger than, for instance, the oscillations that can be obtained by a Hopf bifurcation. Finally, the construction does not depend on the explicit formulation of the equations model and can be applied to a very large class of equations.

A very interesting numerical result shows moreover, in each case, a cascade of period doubling bifurcation of periodic orbits leading to chaos, where the bifurcation parameter is the distance between both reference states.

In a second class of results, we have constructed feedbacks based on the formulas given in [1] in order to get chaos through the construction of homoclinic orbits. Although the formulas are a little bit more complex than before, they do not depend on the specific equations of the initial system and we argue why the chaos that we obtain is structurally stable (thus, can be numerically observed), although the existence of a homoclinic orbit is not a structurally stable property. A difficulty to give evidence of chaos is that the chaotic region can be concentrated in a very thin tubular neighborhood of the homoclinic orbit. Nonetheless, in the real case, two homoclinic orbits are constructed and any sufficiently close orbit follows one or the other separatrix in an unpredictable order, sensitive to initial conditions.

We are considering the possibility of simplifying the nature of the feedback equations by using step-like functions, as in the first class of

systems.

The motivation for the theoretical result in [1] and the work presented here is to develop an innovating therapeutic strategy aiming at breaking homeostasis in agressive organisms. Recall that homeostasis is a fundamental property of living systems: it denotes the ability of an organism to maintain its internal state at equilibrium, while its environment continuously evolves. In general, a default in constancy of one quantity is pathologic. There are plenty of examples. Let us remind the regulation of oxygen pressure in population proliferative cancer cells. When proliferating, they encounter hypoxia conditions in regions which lack blood vessels to bring oxygen. Response genes, like angiogenesis genes, are then activated through transcription factors like *Hypoxia Inducible Factor*, which senses the pressure of oxygen through its hydroxylation sites (see [7], [8]).

The originality of our method relies on the fact that 1) it targets the dynamics of regulation and 2) it acts on the "software" of the organism, inducing a self-disorganization. Moreover, from the work presented here we have learnt that the type of feedback proposed by the method might be very simple: essentially, alternatively positive and negative action on the parameter. This type of action is encountered in natural regulation systems. Figure 15 illustrates the type of regulatory structure which could lead to the desired dynamical behaviour.

As a conclusion, although we are very far from any biological application, we think that the idea deserves enough interest to go on with it.

Aknowledgements We thank F. Dayan for the giving us the idea of the regulatory structure depicted in Figure 15.

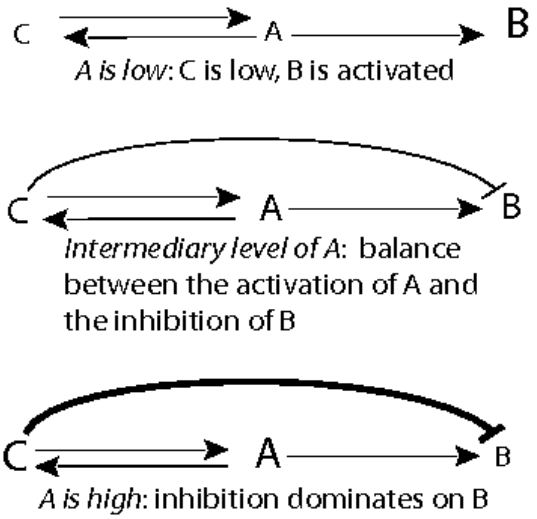

Figure 15: A regulatory structure which could lead to an alternative positive and negative action of the component A onto the component B: A is an activator of B, but its activation saturates for A large; A activates C; when C is above a threshold, C inhibits B

Bibliography

References

[1] 2006 Pécou E., Desynchronization of one-parameter families of stable vector fields *Nonlinearity* **19** 261-76.

[2] 1999 Conrad E., Mathematical Models of Biochemical Oscillations *Thesis*, Virginia Tech.

[3] 1965 Shilnikov L.P., A case of the existence of a denumerable set of periodic motions *Sov. Mat. Dokl.* **6** 163-6.

[4] 1970 Shilnikov L.P., A contribution to the problem of the structure of an extended neighborhood of a rough equilibrium state of saddle-focus typecase *Math. USSR Sb.* **10** 91-102.

[5] 1965 Goodwin B.C., Oscillatory behavior in enzymatic control processes. In Weber, G. (Ed.) *Advances in Enzyme Regulation*, Pergamon Press, Oxford, 425-438.

[6] 1988 Wiggins S., Global Bifurcations and chaos: analytical methods.*Applied Mathematical Sciences* **73**, Springer Verlag.

[7] 2004 Kohn K., et al., Properties of Switch-like Bioregulatory Networks Studied by Simulation of the Hypoxia Response Control System, *Molecular Biol. Cell* **15** 3042-3052.

[8] 2006 Dayan F, et al., The Oxygen Sensor Factor-Inhibiting Hypoxia-Inducible Factor-1 Controls Expression of Distinct Genes through the Bifunctional Transcriptional Character of Hypoxia-Inducible Factor-1A. *Cancer Res.* **66** (7). April 1, 3688-3698